scientific reports

Check for updates

OPEN

Oceanographical-driven dispersal and environmental variation explain genetic structure in an upwelling coastal ecosystem

Lívia Peluso[1,2], Juan Faúndez[7,9], Sergio A. Navarrete[4,6,9,10,11], Bernardo R. Broitman[3,4,5], Christopher M. Aiken[8] & Pablo Saenz-Agudelo[1,6]✉

The seascape comprises multiple environmental variables that interact with species biology to determine patterns of spatial genetic variation. The environment imposes spatially variable selective forces together with homogenizing and diverging drivers that facilitate or restrict dispersal, which is a complex, time-dependent process. Understanding how the seascape influences spatial patterns of genetic variation remains elusive, particularly in coastal upwelling systems. Here, we combine genome-wide SNP data, Lagrangian larval dispersal simulated over a hydrodynamic model, and ocean environmental information to quantify the relative contribution of ocean circulation and environmental heterogeneity as drivers of the spatial genetic structure of two congeneric intertidal limpets, *Scurria scurra* and *S. araucana*, along the central coast of Chile. We find that a genetic break observed in both limpet species coincides with a break in connectivity shown by the Lagrangian dispersal, suggesting that mean ocean circulation is an important seascape feature, in particular for *S. scurra*. For *S. araucana*, environmental variation appears as a better predictor of genetic structure than ocean circulation. Overall, our study shows broad patterns of seascape forcing on genetic diversity and contributes to our understanding of the complex ecological and evolutionary interactions along coastal upwelling systems.

Keywords Seascape genetics, *Scurria*, Chile, Limpets, Southeastern Pacific

Introduction

The environmental, oceanographic and physical features that compose a seascape are spatially and temporally heterogeneous, and can regulate the microevolutionary processes shaping the spatial genetic variation by generating heterogeneous selective forces and variable dispersal[1]. Yet, the role of fluid dynamics together with diverse biological traits in shaping the genetic structure of marine populations remains poorly understood. Seascape genetics aims to fill this gap by quantifying the association between different variables that capture these features. Despite being a relatively recent discipline[2], studies are improving our understanding of how marine populations and ecosystems function and evolve. A key seascape component usually inferred but not quantified is the transport of propagules among sites by ocean currents, since it can lead to both homogenization through high gene flow and divergence by creating temporal dispersal barriers[3]. This advective transport defines patterns and probabilities of connection and temporal isolation among sites[4,5], which explains why genetic breaks are often consistent with ocean circulation breaks[6]. However, estimating and observing ocean circulation at scales relevant for larval dispersal remains challenging, although seascape genetic studies including biophysical simulation data

[1]Instituto de Ciencias Ambientales y Evolutivas, Universidad Austral de Chile, Valdivia, Chile. [2]Escuela de Graduados, Facultad de Ciencias, Universidad Austral de Chile, Valdivia, Chile. [3]Departamento de Ciencias, Facultad de Artes Liberales, Universidad Adolfo Ibáñez, Viña del Mar, Santiago, Chile. [4]Coastal Socio-Ecological Millennium Institute, SECOS, Pontificia Universidad Católica de Chile, Santiago, Chile. [5]Millennium Nucleus UPWELL, Santiago, Chile. [6]Millenium Nucleus for Ecology and Conservation of Temperate Mesophotic Reef Ecosystems (NUTME), Valparaíso, Chile. [7]Departamento de Oceanografía y Medio Ambiente, Instituto de Fomento Pesquero, Valparaíso, Chile. [8]Coastal Marine Ecosystems Research Centre, CQUniversity, Gladstone, Australia. [9]Facultad de Ciencias Biológicas, Estación Costera de Investigaciones Marinas, Pontificia Universidad Católica de Chile, Santiago, Chile. [10]Center for Oceanographic Research, COPAS-COASTAL, Universidad de Concepción, Concepción, Chile. [11]Marine Energy Research and Innovation Energy, MERIC, Estación Costera de Investigaciones Marinas, P. Universidad Católica de Chile, Santiago, Chile. ✉email: pablo.saenzagudelo@gmail.com

have recently become more common[6]. While ocean currents appear to be the primary seascape feature shaping population genetic structure (reviewed in[4,7]), other environmental variables can be important depending on the species studied (e.g.[8–11]). This is because genetic variation in real metapopulations also depends on other biological factors such as mortality in the plankton, availability of suitable habitat, post-settlement survival, and reproductive output, which are in turn modulated by environmental variability and local species interactions[12,13]. The seascape genetics approach has the potential to evaluate both environment and ocean circulation influence, enabling a more complete and useful understanding of how they affect species ecology and evolution.

The Southeast Pacific coast is dominated by the cold Humboldt Current that flows equatorward offshore from around 42°S to around 4°S[14]. Nearshore, the seasonally variable Chile-Peru Coastal current characterizes the coastal ocean[15,16], with velocities that vary alongshore as a result of the interplay between coastal topography and winds[17]. In the central Chilean coast, hydrographic variability and mesoscale coastal circulation patterns are dominated by seasonal and synoptic variation in upwelling-favorable winds[18], which fuel primary productivity by bringing the cold nutrient-rich waters up to the surface. The intensity and persistence of the winds vary along the coast, with comparatively persistent upwelling-favorable winds to the north of 30°S, strong but seasonally variable upwelling winds poleward of this latitude, and strongly seasonal upwelling winds south of 37°S[14,19,20]. A latitudinal gradient in sea surface temperature is observable[21], but with important regional-scale discontinuities[22], and mesoscale variations that also affect primary productivity as inferred from phytoplankton biomass[23–25].

The region around 30°S also marks the distribution limit of many species, both southward and northward, and corresponds to the start of the intermediate or transition area between the Peruvian and Magellanic Provinces[26]. While some invertebrate species do not present obvious genetic structure along most of the Chilean section of the Humboldt current[27–29], others do present a genetic break around the biogeographic limit at 30°S[8,28,30]. For these species, oceanographic and coastal features have been proposed as the drivers of the observed genetic patterns, but no direct connection has been established as yet. Patterns of intertidal community structure, invertebrate recruitment, phenotypic plasticity, and relative intensity of ecological processes also change around this latitude[19,20,26,31–34], highlighting the existence of important changes in the environment.

A useful approach to understanding the effect of the seascape on genetic patterns is studying how the same environmental conditions influence more than one species that inhabit the same space. Comparative studies can help elucidate the causes of common barriers to gene flow. For example, a comparative study of marine fishes with different ecologies in the Mediterranean sea provided evidence of local adaptation driven by temperature in this basin[35]. Additionally, comparative studies can use closely related species, where deep divergent historical factors can be discarded while ecological and life history traits are more similar and comparable. For instance, a study in Hawaii evaluated sympatric limpets with similar life histories that had common seascape drivers to gene flow restriction, such as deep open ocean channels and variable ocean currents[36]. We follow a similar approach here to understand the influence of the Chilean coastal seascape on the spatial genetic variation of two co-occurring limpets, *Scurria scurra* (Lesson, 1830)[37] and *Scurria araucana* (Orbigny, 1841)[38]. These species' ranges overlap for over 18° of latitude (~1300 km)[39], crossing the previously mentioned biogeographic discontinuity at 30°S (BD30). Both limpets inhabit wave-exposed intertidal rocky shores but have distinct habitats. *Scurria araucana* lives directly on rock substrate, while *S. scurra* lives on the stipes of the kelps *Lessonia* spp. and holdfasts of the bull kelp *Durvillaea* spp.[39]. Scarce information is available concerning their reproductive strategies, but the two are gonochoric species and broadcast spawners (L.P. pers. obs.;[39,40]). As observed in other Lottidae[41–44], their larvae are likely lecithotrophic with a short pelagic larval duration of about 10 days and a pre-settlement competent period of 3 to 7 days. These two species and the sympatric *Scurria ceciliana* form a monophyletic group comprising the most recently diverged group within the genus[45]. This relatively recent common ancestry facilitates comparisons of genetic structure to shed light on the effect of the current seascape on the spatial distribution of genetic diversity.

Along the Chilean coast, from ~18 to 53°S, spatial patterns of genetic variation for *S. scurra* and *S. araucana* show a common genetic discontinuity at 32°S[45]. It is unclear whether the discontinuity can be attributed to environmental conditions experienced by benthic animals, or by dispersal and the spatially heterogeneous connectivity generated by ocean circulation. To uncover the underlying processes that shaped spatial genetic variation, we implemented a seascape genomics approach using genomic, environmental and ocean circulation connectivity data. By focusing on the central region of Chile, we used an intermediate-resolution hydrodynamic model that has recently become available and validated[17] to estimate connectivity patterns through the dispersal of Lagrangian propagules. To characterize the environmental components of the seascape, we used remote sensing information, including atmospheric data, since limpets are also exposed and sensitive to atmospheric variables during low tide[32,47]. Considering both limpets have relatively similar life histories, we hypothesize that the patterns and processes of the common seascape they inhabit have similar effects on their genetic variation. Specifically, we tested if subpopulation breaks based on ocean circulation corresponded spatially to the breaks observed with genetic structure and how much mean ocean currents and other environmental features explained genetic variation. With this, we aim to identify broad genetic-environment associations and help uncover the underlying processes that shape genetic connectivity in this seascape.

Methods

Genetic data

Individual genetic data for both *Scurria scurra* and *S. araucana* were obtained from a previously published study[46]. We retrieved RADseq raw reads from samples at six sites between 28° and 34°S in central Chile: Carrizal Bajo (CB), Temblador (TE), Limarí (LI), Huentelauquén (HU), Puertecillo (PU), Concepción (CN) (Fig. 1a). Details from field collections can be found in Table S1. Identification, DNA extraction and RAD sequencing methods are detailed in Peluso et al.[46]. Reads from both species were aligned to the *S. scurra* reference genome[48] (Giles et al., unpublished) for SNP calling using the function *ref_map.pl* in STACKs (v. 2.60)[48]. Only loci present

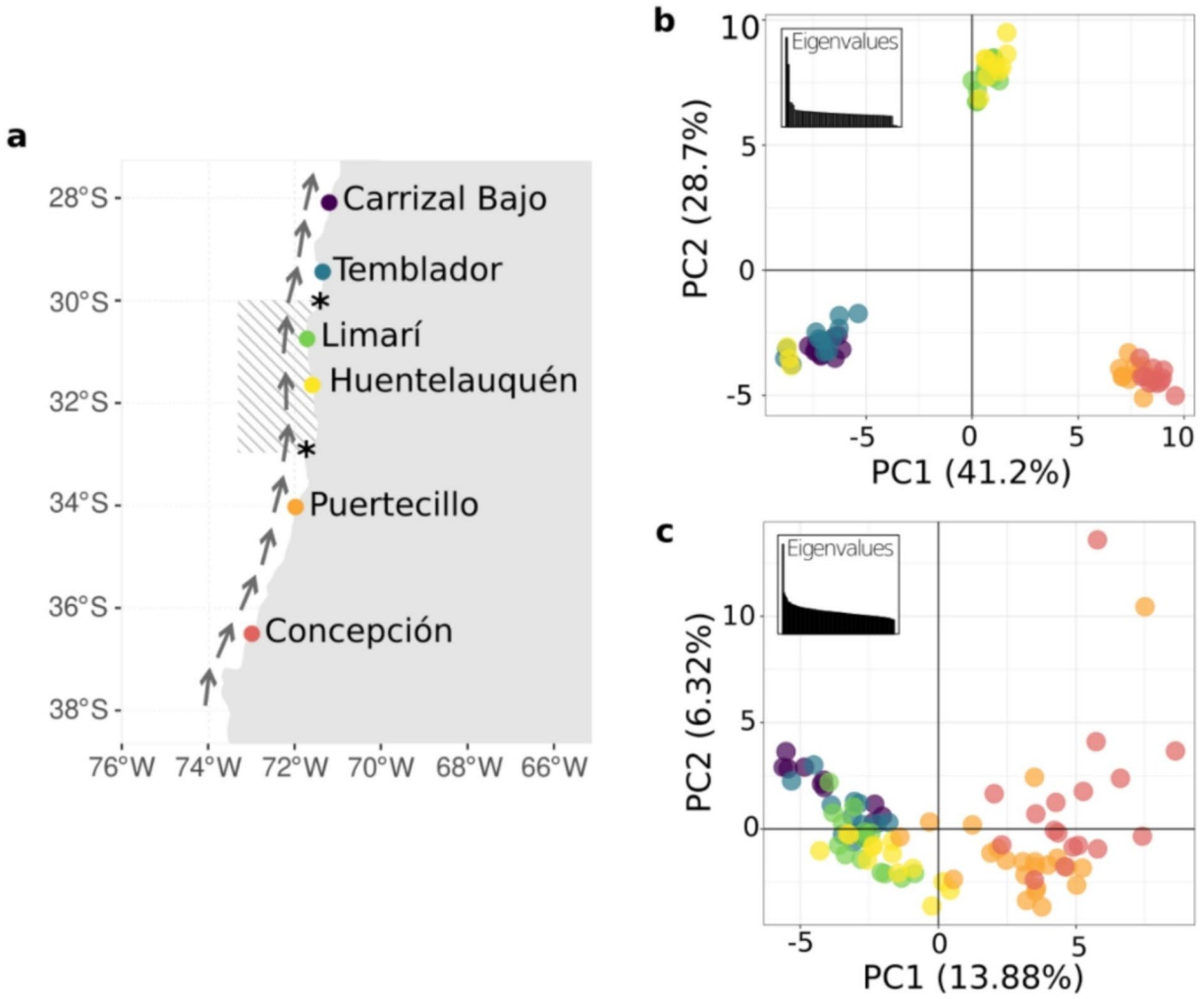

Fig. 1. Map showing the genetic sampling sites, the direction of the surface ocean currents (arrows), the main upwelling centers in the region (asterisks) and the biogeographic limit around 30° S (hatched region) (**a**). Plots showing the first two principal components from the PCA analysis for *S. scurra* (**b**) and *S. araucana* (**c**) using genomic data. Sites are color coded according to the map (**a**).

in at least 80% of samples were considered and only one SNP per locus was kept. SNPs were filtered for mean minimum read depth per locus (15), minor allele count (1), maximum mean depth per site (62–73, depending on the species), and a final genotype call rate of 90% with VCFtools (v. 0.1.16)[49] following O'Leary et al.[50]. Individuals with more than 20% of missing data were removed. SNPs were also filtered for linkage disequilibrium using the function snpgdsLDpruning from the R (v. 4.1.2; R Core Team 2021) package SNPRelate (v. 1.28.0)[51].

Population genetic structure was estimated using two approaches. First, the presence of genetic clusters was evaluated with a principal component analysis (PCA), which was conducted in the R package adegenet (v. 2.1.5)[52]. Secondly, individual ancestry coefficients were estimated with sparse non-negative matrix factorization (sNMF) implemented on the R package LEA (v. 3.6.0)[53], where the number of ancestral populations (k) ranged from 1 to 5 and with 10 repetitions for each k.

Environmental data

Many environmental variables besides ocean currents are expected to influence reproduction, dispersal and recruitment survival of *Scurria* limpets, which in turn shape their genetic diversity. In order to better characterize such seascapes, we used seawater and atmospheric variables retrieved from satellite data. For seawater variables, salinity, mean nitrate concentration, mean phosphate concentration and the annual minimum and maximum of monthly climatologies for sea surface temperature were retrieved from the Bio-ORACLE database[54]. The variables chosen include extremes of surface temperature and salinity, factors that can influence larval dispersal, mortality, and also settlement by creating fronts and acute stress gradients. We also included nutrients concentration that influence algal growth, hence adult limpets' nutrition, a factor that presumably determines reproduction success. For atmospheric variables, the mean temperature of the warmest quarter, the mean temperature of the coldest quarter, and annual precipitation were obtained from the WorldClim database[55]. The variables chosen likely

influence species survival and reproduction, considering the limpets are exposed to atmospheric changes during low tides. To retrieve these variables, the function load_layers from the R package *sdmpredictors* (v. 0.2.11)[56] was used to access the environmental layers, and the function *extract* from the R package *raster* (v. 3.5–11)[57] was used to get the values corresponding to the genetic sampling sites.

Ocean circulation data

We configured a biophysical simulation fed by ocean velocity fields produced by a hydrodynamic model of the studied area to estimate dispersal based on ocean circulation alone. The ocean velocity fields were retrieved from a climatological simulation of the ocean circulation in central Chile[17] performed using the Coastal and Regional Ocean Community model (http://www.croco-ocean.org). This hydrodynamic model domain extended between 27–39°S and 70–83°W with a horizontal resolution of 8 km (1/12°) and a vertical resolution of 40 sigma levels. This model was forced with a climatological wind stress from Scatterometer Climatology of Ocean Winds (SCOW, 2000–2008)[58] and with boundary conditions obtained from the Simple Ocean Data Assimilation (SODA, 1958–2008) reanalysis[59]. The hydrodynamic model grid was interpolated horizontally from C- to A-type grid and vertically from sigma to zeta levels before being used for the biophysical simulations of propagule dispersal.

The Connectivity Modeling System (CMS) was used for tracking the propagules released in the ocean velocity field, which implements a multiscale stochastic Lagrangian framework[60]. To determine particle release and settlement locations, 31 polygons were defined within the hydrodynamic model boundary avoiding the edges. We used $939.45 \pm 23{,}73$ km^2 polygons encompassing approximately 40 km of shoreline (Fig. S1). Lagrangian simulations were set up with the flag for looping through the velocity fields set to "true" in the "runconf.list" file from CMS, which allows repeat cycles from only six climatological years available from the hydrodynamic model[17]. The flag landmask boundary condition to avoid the coast was also set to "true" in order to prevent particle stranding. Since the horizontal resolution of the used hydrodynamic model does not fully capture the nearshore circulation, turbulence from a nested model with considerably higher resolution (0.5 km) described by Faúndez et al.[17] was added to increase particle randomness and to represent subgrid-scale motion. For this, a horizontal diffusivity of 0.025 m^2/s^2 and a vertical diffusivity of 0.016 m^2/s^2 were included in the flag turbulence module in CMS. Particles were released from different positions inside each polygon, and release occurred at the surface twice a month for 30 years (i.e., 6 years x 5 cycles), with 252,000 particles released within each polygon and 7,812,000 particles released across the region. Based on estimates from other patellogastropods[41–43], larval pre-competency period, i.e. the minimum age the particle was allowed to have before settling ("settlementStart"), was set to 3 days. Considering the pelagic larval duration (PLD) is not known for these species, we tested different values within the known range for other limpets in the family Lottidae[41–44]. With this, different values of maximum advection time for particles ("timeMax") were tested corresponding to 5, 10 and 20 days (PLD5, PLD10 and PLD20, respectively).

Biophysical simulations from CMS were run in the supercomputer Guacolda-Leftraru from the National Laboratory for High-Performance Computing in Chile (NLHPC; https://www.nlhpc.cl/). From particle tracking outputs, a connectivity matrix was generated using the Matlab (The MathWorks, Inc.) script "make_mtx.m" provided by CMS. Because we were interested in the dispersal probability rate, the connectivity matrix was divided by the reproductive output[61], which corresponds to the total number of particles released in each polygon. Self-recruitment (SR), defined as the proportion of recruitment of one site that corresponds to individuals born in that site, as well as local retention (LR), defined as the proportion of particles released at one site that also recruited in that site[61,62] were calculated for the three PLDs using the R package ConnMatTools (v. 0.3.5)[63].

Ocean circulation connectivity

The connectivity pattern of ocean circulation among sites is often complex and often results in locales (polygons) that are highly and frequently connected with others, but scarcely and infrequently connected with the rest[64]. These varying rates of connectivity thus define gene flow driven by ocean circulation. Subpopulation structure is not always evident simply by visualizing the connectivity matrix. To verify if breaks among locations based on ocean circulation geographically coincided with the breaks observed in genetic structure, we applied two methods to determine the existence of subpopulations due to ocean circulation alone. Both were based natively on the connectivity matrices, not their graph representations.

The first method was proposed by Jacobi et al.[64] and is based on the compartmentalization schemes from graph theory applied to probabilities of the connectivity matrix that usually results from a single reproductive event or, in our case, from running the model for 30 years. The approach consists of recursively splitting and merging locales (polygons) to minimize dispersal among subpopulations and maximize dispersal within groups of locales, i.e. subpopulations. Calculations were done using the function optimalSplitConnMat from the ConnMatTools R package.

The second approach to estimating subpopulations, proposed by Aiken and Navarrete[4], considers the connectivity over multiple generations, as is appropriate for gene flow. Subpopulation partitions are thus defined based on the number of generations (tau) that separate each pair of sites, and a limiting probability of connection (phi). Such limiting probability (phi) can also be visualized as connectivity uncertainty; for instance, dispersal connections with small values, such as 20 particles over 30 years, have little impact on metapopulation dynamics or effective gene flow. The limited impact of small connectivity values is compounded by the fact that biophysical simulations do not account for important biological parameters, for instance post settlement mortality and larval behavior, hence overestimating reproductive connectivity. In our case, and in the absence of a specific evolutionary model, we considered only the connections where the number of particles was higher than 0.1% of the overall settled particles (around 2000 particles). Partitioning calculations were made for phi ranging from 0 to the set value and for generational times (tau) ranging from 1 to 10 generations. Analyses were run in R using the YASS algorithm provided by the authors[4].

Seascape dataset

To understand the seascape's role in genetic diversity, we wanted to establish how much geography, ocean circulation and the environment explain variation in the genetic data. For geography data, only the latitude of sampling sites was used. This is because using MEMs based on overwater distance or including longitude gives the same result (results not shown), but add more variables to the seascape dataset. For ocean circulation and environmental variables that represent complex and sometimes inter-dependent attributes of the seascape, we first reduced its complexity and removed redundancy due to cross-correlation using different methods. In the environmental dataset, multiple variables were highly collinear (Pearson correlation > 0.75), e.g. nitrate and phosphate concentration, salinity and sea surface temperature variables (Table S2), and we used principal components analysis (PCA) to reduce dimensionality. Correlations were calculated using the function pairs.panels of the R package psych (v. 2.1.9)[65] and the PCA with the function prcomp from the R base package stats with centering and scaling of variables. We retained the first two principal components (PCs) for the subsequent analyses.

For the ocean circulation data, complexity reduction involves more dimensions as it represents directional and potentially non-Euclidean alongshore processes in space. We used a method called asymmetric eigenvector map (AEM) developed by Blanchet et al.[66] to model the multivariate spatial relationship among locations generated by an asymmetric, directional process, in our case the flow of nearshore currents. This method consists of constructing eigenvectors based on the singular-value decomposition of a weighted site-by-edges asymmetric matrix, which represents all studied sites (nodes) and a weighted connection diagram (edges) between them, which is given by the ocean circulation connectivity matrix in our case. With this, we generated vectors that could be directly used with the PCs from the environmental dataset as explanation variables to test relationships with genetic variation. First, we used the PLD10 connectivity matrix considering only the six genetic sites and whenever the probability of connection was greater than 0, the pair of sites was kept as an edge in the matrix. Using these connections as edges and site coordinates, we built a site-by-edges matrix with the function aem.build.binary from adespatial (v.0.3–14)[67]. In the diagram generated (Fig. S2) the upstream site was added in the south, according to the main ocean circulation pattern in the region that flows northward (Fig. 1a), and connections to this site were later removed. Besides, to ensure there are no loops, when there were connections in both ways between sites only the direction of higher dispersal probability was kept. Using this site-by-edges matrix we calculated the AEMs with the function aem (adespatial) using the dispersal probability rates from the connectivity matrix as weights.

Seascape genetics analyses

To understand the influence of the seascape in genetic variation, we used redundancy analyses (RDA) with the seascape dataset as explanatory variables and the genetic dataset as SNPs allele count matrices as response variables. In this genetic dataset, 0 corresponds to the homozygous for the reference allele, 1 corresponds to the heterozygous, and 2 corresponds to the homozygous for the alternate allele. Missing values were replaced by the most common genotype overall.

We ran a model with all seascape variables for each species with the function rda from the package vegan (v. 2.5-7)[69]. Models were tested for significance with the function anova.cca from vegan with 999 permutations. If the models were significant, the forward selection approach with the two-stopping criteria proposed by Blanchet et al.[68] was used. We did this to obtain a subset of seascape variables and avoid model overfitting considering the number of variables and the number of sampling sites is similar. This was applied with the function ordiR2step from vegan with 999 permutations. Variables were selected based on the permutation test results, with p-values adjusted with Holm's correction with the function p.adjust from stats (R Core Team 2022).

To understand the separate contribution of geography (lat), ocean circulation (AEM vectors) and environment (PC) in explaining genetic variation, we used partial RDA (pRDA) since they can show the proportion of variance explained by one set of variables excluding the effect of the other variables (covariables). For this, the models with the selected seascape variables were considered as the full models and pRDA were run to understand the separated effect of geography, ocean circulation and environment. Three models were tested for each species, where each set of seascape variables (geography, ocean circulation, environment) was used as explanatory variables (X) and the others were used as covariables (W) using the rda function (vegan). Models were tested for significance with the function anova.cca (vegan) with 999 permutations.

We used the RDA to test for genetic-environment associations using the genetic and the seascape datasets. For this, we retrieved the SNPs loadings (scores) for the significant constrained axes in the ordination space from the results of the previously described full model RDA[70]. Using a histogram of the loadings we considered the tails of the distribution as indicators of significant relationships with the explanatory variables and, therefore, candidate SNPs to be under selection. The loadings were selected using a standard deviation cutoff of 3.5. The relationship between each selected SNP and a seascape variable was defined based on the highest correlation coefficient.

Results

Genetic structure

The dataset with all loci for *S. scurra* consisted of 28,277 SNPs genotyped for 68 individuals and for *S. araucana* of 21,207 SNPs genotyped for 92 individuals. For *S. scurra*, PCA analysis shows three clearly distinct groups (Fig. 1b). The sNMF analysis suggests four populations but the barplots revealed that three groups are the predominant feature (Fig. S3), with three individuals from the northern group clustering with the central one. For *S. araucana*, PCA analysis reveals two groups with a slight continuous differentiation between sites (Fig. 1c) and sNMF identified only one population, yet inspection of the barplots suggested the presence of at least two (Fig. S4). The spatial patterns of genetic variation in both species showed a break between Huentelauquén (HU) and Puertecillo (PU) sites, while another break was observed between Temblador (TE) and Limarí (LI) only for *S. scurra*.

Ocean circulation modeling

The patterns of connectivity observed with the ocean circulation models showed that settlement occurred preferentially equatorward (downstream) of the source site, under the influence of the prevailing northward flow along the Chilean coast. A slight increase in dispersal range was observed with increasing PLD (Fig. 2). There was little difference in the number of particles that settled in relation to the number of particles released among the three PLDs tested with 23.4% in the model with PLD5, 26.3% with PLD10 and 27.2% with PLD20. Considering the coastal polygons as representatives of genetic sampling sites, self-recruitment was larger in LI and HU, while TE had higher values of relative local retention for all three PLDs (Table S3). The remaining sites, Carrizal Bajo (CB), PU and Concepción (CN), had low values of self-recruitment and local retention (Table S3).

Ocean circulation connectivity

We found a number of coincident barriers in the subpopulations calculated, while some differences were found between methodologies. Subdivisions based on ConMatTools[64] were the same, independent of PLD, and the number of optimal splits varied from 2 to 4 (Fig. 3a). A barrier between HU and PU was present with all three optimal splits, and a further subdivision was observed in the southern region with 3 and 4 splits (Fig. 3a). The subdivision analysis using the YASS algorithm[4] showed that all sites eventually get connected when phi = 0 and clusters were observed until the number of generations (tau) reached five (Fig. S5). For the three PLDs tested and considering only dispersal connections above the threshold probability of phi ≈ 0.01, several subpopulations were apparent for connections over a single generation (tau = 1). After three generations (tau ⩾ 3), we observed three subpopulations (Fig. 3b) and three subdivisions for all PLDs tested when phi = 0.01 (Fig. S5).

Seascape dataset

The first two PCs from environmental data (named satPC1 and satPC2), explaining 94.5% of the variance. satPC1 represented mainly the covariance of salinity, maximum seawater temperature and precipitation and satPC2 represented the covariance between atmospheric warmest temperature and minimum seawater temperature (Fig. S6).

The AEM methodology generated three vectors, referred to as currAEM1, currAEM2 and currAEM3. The vectors currAEM1 and currAEM2 appear to reflect large scale effects and separate the southern sites HU, PU and CN from the northern sites CB, TE and LI, with currAEM2 showing an additional separation between LI and the other sites (Fig. S7). The vector currAEM3 shows small scale effects, with differentiation only among CB, TE and the other sites (Fig. S7).

Seascape genetics analyses.

For *S. scurra*, the model with all seascape variables was significant and the forward selection procedure selected the variables lat, currAEM1, currAEM2 and satPC2. The RDA with these variables (full model) explained 11% of the genetic variance in *S. scurra* (Table 1; Fig. 4a). The influence of the different seascape factors estimated by the pRDA showed that ocean currents (currAEM1, currAEM2) and geography (lat) had the larger effects on genetic variation even after controlling for the effect of other seascape variables, explaining 42% and 29% of the full model variance, respectively (Table 1). The remaining variance of the full model was explained by the environment (15%) and the confounded effect of the seascape variables (14%). The genetic-environment association analysis made with the full model RDA scores detected 864 candidate loci. From these, the majority are either associated with the variables lat ($n = 475$) or currAEM2 ($n = 369$) (Fig. 4c).

For *S. araucana*, the model with all seascape data was also significant and the selected variables were lat, currAEM2, satPC1 and satPC2. The RDA with these selected variables (full model) explained 3% of the genetic variance in this species (Table 2; Fig. 4b). The proportion of variance explained by each seascape factor estimated by the pRDA showed a higher influence of the environment (satPC1, satPC2), which explained 33% of the full model variance, and also a similar amount of variance explained by the confounded effect of the seascape variables. Geography and ocean currents explained a smaller proportion of the full model variance. The genetic-environment association analysis made with the full model RDA scores identified 629 candidate loci. Almost half of these outliers are associated with lat ($n = 307$) and the rest are mainly associated with satPC1 ($n = 124$) and currAEM2 ($n = 122$) (Fig. 4d). (Table 2).

Discussion

The genetic structure pattern for both limpets, *Scurria scurra* and *S. araucana*, showed a common discontinuity between Huentelauquén (HU; 31.6°S) and Puertecillo (PU; 34.1°S) sites (Fig. 3c) that coincided with the subdivision obtained based solely on ocean circulation connectivity, where we observed one to two breaks (Fig. 3a, b). These ocean circulation breaks were detected with the three biophysical settings, corresponding to pelagic larval durations of 5, 10 and 20 days, suggesting low variability in particle transport in this area within this larval duration range. Such concordance between genetic and oceanographic patterns indicates that advection alone could explain this common genetic cline, likely creating a natural and sufficiently persistent dispersal barrier in this region for these limpets and possibly for other organisms with similar larval dispersal traits. Indeed, a genetic discontinuity around 31–34°S has been observed in another *Scurria*, S. *zebrina*[71], and the tunicate *Pyura chilensis*, which has larval development of just a few day[30,72,73]. This advective barrier could be related to the two main upwelling centers in Chile that occur in the region, one in Coquimbo (Punta Lengua de Vaca, 30°S) and the other in Valparaíso (Punta Curaumilla, 33°S)[16]. Still, it is important to consider that the modeled biophysical dispersal estimated here does not realistically simulate the near-shore ocean circulation within the coastal boundary layer, such that the realized dispersal is likely more complex. Nonetheless, the results unambiguously indicate the existence of a sufficiently persistent barrier to dispersal that occurs between 31–34°S, driven by the regime of ocean currents that consistently limit the exchange of individuals across this region.

The importance of ocean circulation in shaping the genomic variation in *S. scurra* and *S. araucana* is further corroborated by the seascape genetic analyses. These showed that ocean circulation variables were important in explaining the genetic variation of both limpets, especially in *S. scurria*. For this limpet, ocean circulation was the seascape feature that better explained genetic variation even when controlled for the other seascape features.

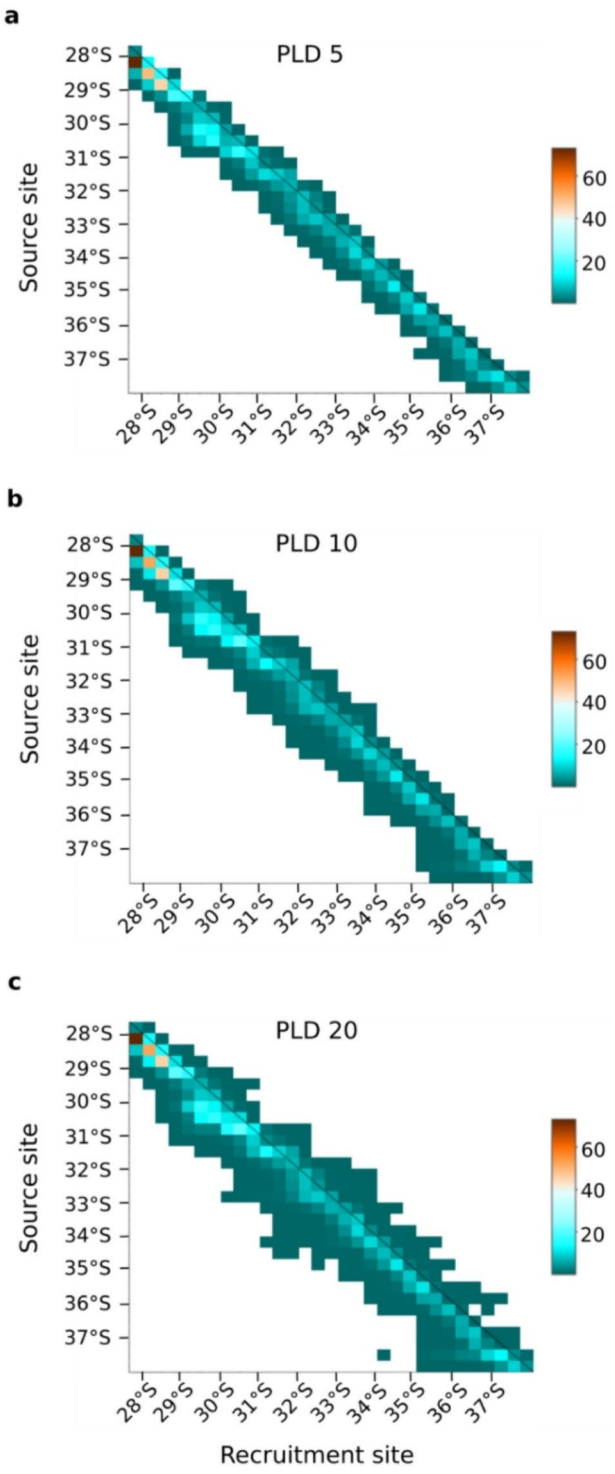

Fig. 2. Plots showing the connectivity matrices for the different pelagic larval durations modeled, PLD5 (**a**), PL10 (**b**), and PLD20 (**c**).Source sites are given in the y axis while x axis shows recruitment sites. The color bar represents the percentage of settlers arriving at a site in relation to the released particles. Zeros are represented in white.

The genetic-environment association analyses further evidenced the importance of ocean circulation for these species since many candidate loci were associated with these variables. For *S. scurra* 44.2% of the candidate loci are related with ocean circulation (currAEM1, currAEM2) while for *S. araucana* ocean circulation (currAEM2) is associated with approximately 19.4% of the detected outliers. Thus, these observations corroborate the existence

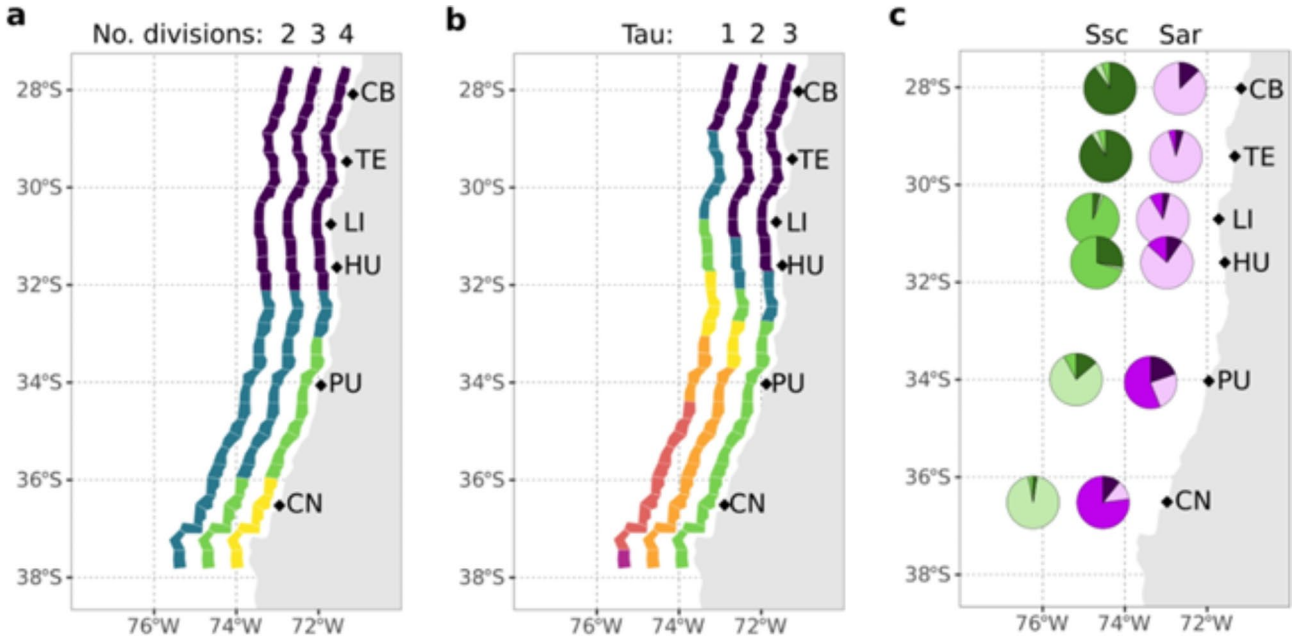

Fig. 3. Maps showing the spatial subdivisions based on the ocean currents connectivity and genetic connectivity. For ocean currents connectivity, subdivision was based on ConnMatTools (**a**) and YASS (**b**) algorithms considering PLD10. For genetic connectivity (**c**), the best number of populations (k) was determined by sNMF and PCA. The pie charts show the mean admixture proportions in each site considering the selected k for each species.

Partial RDA models	Adj.R^2	Inertia	Prop. explainable variance	Prop. total variance	Pr(> F)
Full model: genSsc ~ lat + currAEM1 + currAEM2 + satPC2	0.108	306.07	1.000	0.16	0.001
Geography: genSsc ~ lat + Condition (currAEM1 + currAEM2 + satPC2)	0.036	89.91	0.294	0.05	0.001
Ocean circulation: genSsc ~ currAEM1 + currAEM2 + Condition (lat + satPC2)	0.042	128.31	0.419	0.07	0.001
Environment: genSsc ~ satPC2 + Condition (lat + currAEM1 + currAEM2)	0.011	45.46	0.149	0.02	0.001
Confounded geography/ocean currents/ environment		42.39	0.139	0.02	
Total unexplained		1595.33		0.84	
Total inertia		1901.40		1.00	

Table 1. Partial redundancy analysis (pRDA) results showing the influence of geography, ocean currents and environment on *S. Scurra* genetic variation. For both species, the full models use the selected seascape variables from forward selection. Seascape variables were divided in geography (lat), ocean circulation (currAEM1, currAEM2), and environment (satPC2). The proportion of explainable variance corresponds to the proportion explained by each pRDA considering the total constrained variation explained by the full model.

of at least partial barriers to dispersal driven by ocean circulation and consequent independent adaptations. On the other hand, geography was associated with the majority of outliers in *S. scurra* (55.0%) and *S. araucana* (48.8%). For *S. araucana*, the environment (satPC1, satPC2) also played an important role in genetic variation and it was associated with 31% of the outlier loci. Considering the correlation of satPC1 with latitude observed for *S. araucana*, and also the amount of variance explained by the confounded effect among the seascape variables for both species, the candidate loci found could reflect adaptations to an environment gradient that follows latitudinal change, which can be strengthened by limited gene flow across this barrier. In fact, a discontinuous latitudinal gradient pattern along the Chilean coast has been reported for many environmental components, like chlorophyll-a, air temperature, precipitation, freshwater inflow and seawater temperature (e.g.[16,21,22,74]). Although the effect of ocean circulation on dispersal and consequent population connectivity appears to play a major role in shaping these limpets' genomic variation, there is likely an environmental differentiation caused by the patterns of ocean circulation that affect the sorting of larvae, which remains to be experimentally tested.

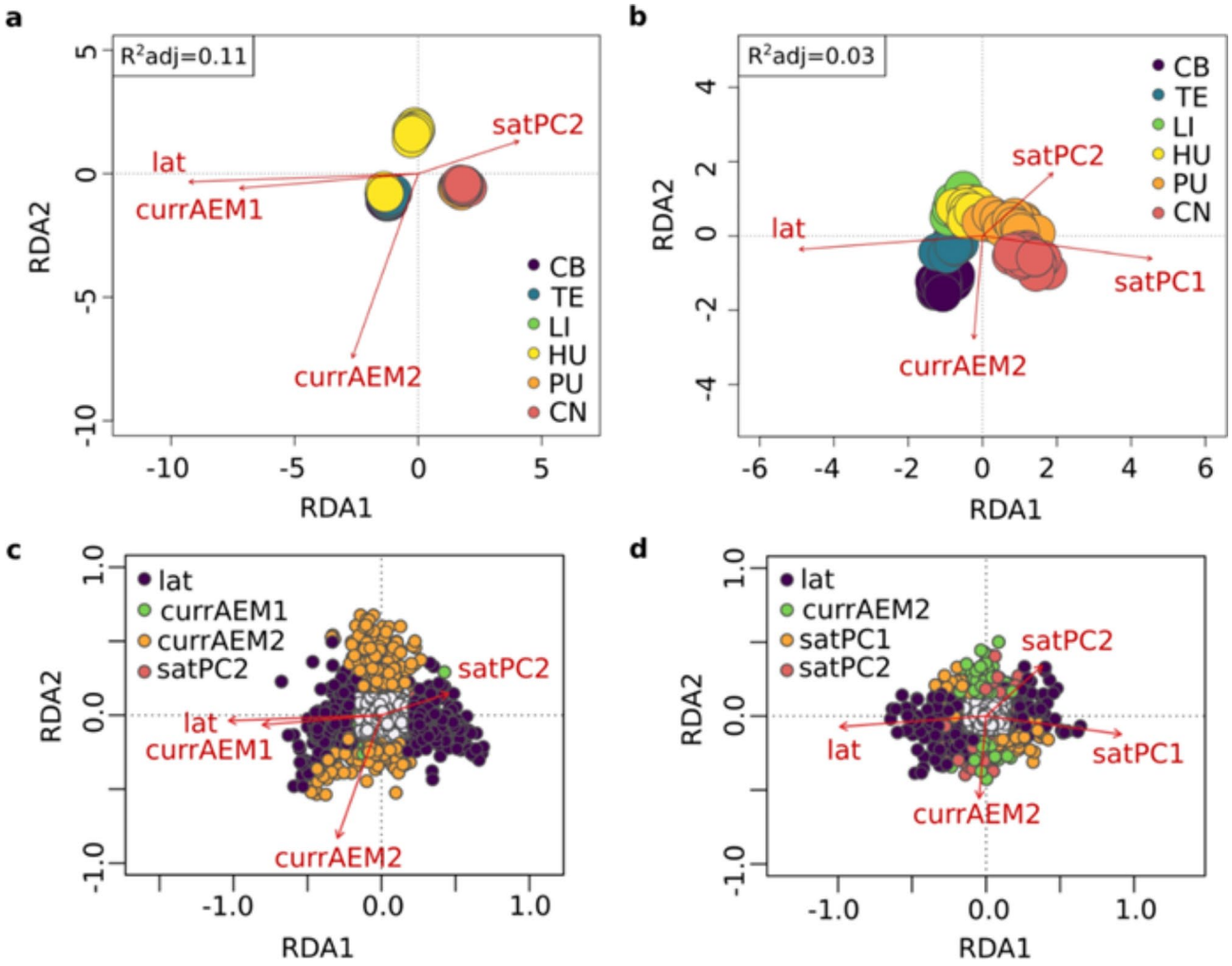

Fig. 4. RDA plots showing the relationship of the selected seascape variables with the genomic datasets of *S. scurra* (**a**) and *S. araucana* (**b**). SNPs are shown in gray and individuals are colored according to their sampling sites. The results of the genetic-environment association made in these RDA-ordinated spaces is also given for *S. scurra* in (**c**) and *S. araucana* (**d**), where the distribution of the candidate SNPs (colored) can be seen.

Partial RDA models	Adj.R^2	Inertia	Prop. explainable variance	Prop. total variance	Pr(> F)
Full model: genSar ~ lat + currAEM2 + satPC1 + satPC2	0.032	97.88	1.00	0.07	0.001
Geography: genSar ~ lat + Condition (currAEM2 + satPC1 + satPC2)	0.002	16.25	0.166	0.01	0.001
Ocean circulation: genSar ~ currAEM2 + Condition (lat + satPC1 + satPC2)	0.002	16.54	0.169	0.01	0.001
Environment: genSar ~ satPC1 + satPC2 + Condition (lat + currAEM2)	0.003	32.36	0.331	0.02	0.001
Confounded geography/ocean currents/ environment		32.73	0.334	0.02	
Total unexplained		1218.00		0.93	
Total inertia		1316.00		1.00	

Table 2. Partial redundancy analysis (pRDA) results showing the influence of geography, ocean currents and environment on *S. araucana* genetic variation. For both species, the full models use the selected seascape variables from forward selection. Seascape variables were divided in geography (lat), ocean circulation (currAEM2), and environment (satPC1, satPC2). The proportion of explainable variance corresponds to the proportion explained by each pRDA considering the total constrained variation explained by the full model.

This shows that this seascape also has an important environmental filter, yet, given the covariation between the environment, ocean circulation and geography, the individual effect of these multiple variables on genetic structure could not be separated.

Along the entire Chilean coast (18–55°S), two biogeographic provinces are broadly recognized: the Peruvian Province and the Magellanic Province[75]. More recently, the intermediate northern-central region has been classified as a transition zone named the Intermediate Area (IA)[26], with further subdivisions proposed based on physical processes [76]. The most intensively studied biogeographic limit is BD30 - in the equatorward range of the IA around 30°S. This 30°S limit is usually associated with changes in oceanographic conditions and is the distribution limit of many species[26]. Indeed, a recent biogeographic study based on community composition of intertidal invertebrates found two breaks around the IA depending on larval development modes, one at 30°S and another at 35°S[21]. Although the Lara et al.[21] results do not apply directly to *Scurria* limpets as their ranges span these two breaks, they likely represent dispersal barriers since a genetic discontinuity was also found for *S. scurra* further north between Temblador (TE; 29.5°S) and Limarí (LI; 30.8°S) sites. Genetic breaks have also been found for other invertebrates that cross the area around 30°S, such as *Notochthamalus scabrosus*[29] and *Crepipatella dilatata*[77]. Yet, many other studies that show a genetic break at the IA did not have the spatial resolution for pinpointing its location at 30°S or 35°S (e.g.[28,78,79]), and the observed genetic breaks might overlap with the previously discussed barrier found here at 31–34°S. Our results indicate that studies with intense spatial sampling design are needed to better understand the location of the genetic discontinuities in this region[80]. Since the subdivisions based on population connectivity via oceanic dispersal showed only transient breaks around 30°S and with just one of the methodologies used (YASS; Fig. 3), our results suggest this break may be related to other seascape features besides or in addition to ocean current flows, for species with similar short larval duration.

Our two focal *Scurria* are sympatric along a large section of their geographic range, so they share local environmental variability patterns. Although they have a common break and common seascape drivers as discussed above, the genomic diversity patterns are substantially different. While *S. scurra* showed an additional genetic break further north at around 30°S and a more marked genetic structure among populations, *S. araucana* showed patterns consistent with higher gene flow. For the later species, the environment appears to have a greater contribution than ocean currents in explaining genetic variation, which is consistent with the observed latitudinal gradient of environmental features and the gradual increase in genetic variation with latitude. The different genetic patterns between the species are evident when considering the more accentuated change in allele frequencies observed for *S. scurra* populations across the common break at 31–34°S. The restricted gene flow imposed by ocean currents appears to be more important in determining this species' genetic variation, which could be further enhanced by other seascape or habitat constraints. Distinctions in physiology or ecology between these two limpets could explain the genetic patterns observed. For instance, differences in physiological responses to heat stress have been observed for populations of two other congeneric species, *S. zebrina* and *S. viridula*, depending on the proximity of the 30°S range edge[32]. However, to our knowledge, there are no studies addressing the physiology of the *Scurria* investigated here, nor on physiological tolerances of their larval stages. Nonetheless, these results indicate that seascape effects are not homogeneous between the co-occurring limpets considered here.

The greater influence of the seascape on *S. scurra* compared to *S. araucana* could be related to their habitat differences, particularly because *S. scurra* is specialized for life onto and feeding on kelp fronds. One possibility is that kelp species influence effective dispersal, recruitment, and/or survival of *S. scurra* limpets. For instance, the northern genetic break observed for *S. scurra* coincides with a similar range limit in kelp distribution; equatorward of 30°S only *Lessonia berteroana* occurs, and south of 30°S *Lessonia spicata* and *Durvillaea incurvata* coexist[81–83]. It is possible that local adaptation to different algal hosts has evolved. This idea seems to be supported by the high number of outlier loci observed in *S. scurra*, but this remains to be experimentally tested. Previous studies have shown that *Durvillea* is highly buoyant and could facilitate the dispersal of *S. scurria* via rafting[84]. This kind of dispersion is in agreement with our previous study that described genetic homogeneity for *S. scurra* southern populations going from Puertecillo (34.1°S) to Magallanes (53.6°S)[46]. Finally, the break at 31–34°S appears more puzzling. We speculate it could also be associated with an interaction between local adaptation to *Lessonia spicata* and this particular region's unique environmental and oceanographic conditions[21]. Alternatively, an edge effect could account for higher selection pressure leading to the high genomic differentiation observed in this region[85]. These scenarios are not mutually exclusive, but further physiological and ecological studies are needed to verify them.

Our results show that the flow patterns of ocean circulation are an important seascape factor shaping genomic variation in two *Scurria* species and most likely for other organisms with similar life histories, especially around the break observed at 31–34°S. Studies with more fine-scale sampling are needed to determine the exact location of breaks in this biogeographic transition area and to understand how they affect different organisms. The results obtained also highlight the importance of advective processes in the ecology and evolution of these limpets, and indicate that ocean current flows are an essential factor to understand seascape genetics for marine organisms with low to moderate dispersal, but that the resulting genetic structure emerges from the interaction between advective process and local selective factors. These results should also offer a good basis for understanding ocean current connectivity breaks in the coast for other species with similar distribution and life histories. Besides, the difference observed between limpets shows that specific ecological particularities can lead to different microevolutionary processes shaping genomic variation even under the influence of the same environmental conditions. This emphasizes how the central region of the Chilean coast presents a good model system to understand genomic differentiation following the restricted dispersal patterns maintained by advective processes, as estimated here, and also how environmental gradients could lead to local adaptation. With this, we demonstrate the seascape forcing of population structure for two sympatric intertidal limpets and

hope it will be a primary groundwork for understanding how species' ecology and evolution are shaped by the seascape they live in.

Data availability

For genetic data, raw individual fastq files can be found at the NCBI SRA repository under the bioproject number PRJNA944965. Filtered VCF files used in the analyses, as well as the connectivity matrix derived from the biophysical models and the environmental variables used can be found at Figshare (10.6084/m9.figshare.c.7357234).

Received: 12 April 2024; Accepted: 11 September 2024
Published online: 20 September 2024

References

1. Liggins, L., Treml, E. A. & Riginos, C. Seascape genomics: Contextualizing adaptive and neutral genomic variation in the ocean environment. In *Population genomics: marine organisms* (eds Oleksiak, M. & Rajora, O.) 171–218 (Springer, 2019).
2. Selkoe, K. A., Henzler, C. M. & Gaines, S. D. Seascape genetics and the spatial ecology of marine populations. *Fish. Fish.* **9**, 363–377 (2008).
3. Treml, E. et al. Reproductive output and duration of the pelagic larval stage determine seascape-wide connectivity of marine populations. *Integr. Comp. Biol.* **52** (4), 525–537 (2012).
4. Aiken, C. M. & Navarrete, S. A. Incorporating the connectivity timescale in metapopulation partitioning. *Am. Nat.* **196** (2), 145–156 (2020).
5. Siegel, D. A. et al. The stochastic nature of larval connectivity among nearshore marine populations. *P Natl. Acad. Sci. USA.* **105** (26), 8974–8979 (2008).
6. Jahnke, M. & Jonsson, P. R. Biophysical models of dispersal contribute to seascape genetic analyses. *Philos. Trans. R Soc. B.* **377**, 20210024 (2022).
7. Selkoe, K. A. et al. A decade of seascape genetics: contributions to basic and applied marine connectivity. *Mar. Ecol. Prog Ser.* **554** (1), 1–19 (2016).
8. Ewers-Saucedo, C. et al. The oceanic concordance of phylogeography and biogeography: a case study in *Notochthamalus*. *Ecol. Evol.* **6** (13), 4403–4420 (2016).
9. Nanninga, G. B., Saenz-Agudelo, P., Manica, A. & Berumen, M. L. Environmental gradients predict the genetic population structure of a coral reef fish in the Red Sea. *Mol. Ecol.* **23** (3), 591–602 (2014).
10. Saenz-Agudelo, P., Dibattista, J. D., Piatek, M. J. & Michelle, R. Seascape genetics along environmental gradients in the Arabian Peninsula: insights from ddRAD sequencing of anemonefishes. *Mol. Ecol.* **24**, 6241–6255 (2015).
11. Selkoe, K. A. et al. Taking the chaos out of genetic patchiness: seascape genetics reveals ecological and oceanographic drivers of genetic patterns in three temperate reef species. *Mol. Ecol.* **19**, 3708–3726 (2010).
12. Cowen, R. K. & Sponaugle, S. Larval dispersal and marine population connectivity. *Annu. Rev. Mar. Sci.* **1**, 443–466 (2009).
13. Watson, J. R. et al. Realized and potential larval connectivity in the Southern California Bight. *Mar. Ecol. Prog Ser.* **401**, 31–48 (2010).
14. Strub PT et al. 1998 Coastal ocean circulation off western South America. In: Robinson AR, Brink KH (eds) *The Sea.* John Wiley, 273–313
15. Aiken, C. M., Navarrete, S. A., Castillo, M. I. & Castilla, J. C. Along-shore larval dispersal kernels in a numerical ocean model of the central Chilean coast. *Mar. Ecol. Prog Ser.* **339**, 13–24 (2007).
16. Thiel, M. et al. The Humboldt Current System of northern and central Chile oceanographic processes, ecological interactions and socioeconomic feedback. *Oceanogr. Mar. Biol.* **45**, 195–344 (2007).
17. Faúndez, J., Acary-Robert, C., Aiken, C., Rousseau, A. & Navarrete, S. *Circulation Variability inside the Coastal Boundary Layer along the Upwelling off Central Chile Solved in a high-resolution Model [Manuscript Submitted for Publication]* (Facultad de Ciencias Biológicas, Pontificia Universidad Católica de Chile, 2022).
18. Aguirre, C. et al. Recent changes in the low-level jet along the subtropical west coast of South America. *Atmos.* **12** (4), 465 (2021).
19. Navarrete, S. A., Wieters, E. A., Broitman, B. R. & Castilla, J. C. Scales of benthic–pelagic coupling and the intensity of species interactions: from recruitment limitation to top-down control. *Proc. Natl. Acad. Sci. U S A.* **102** (50), 18046–18051 (2005).
20. Navarrete, S. A., Barahona, M., Weidberg, N. & Broitman, B. R. Climate change in the coastal ocean: shifts in pelagic productivity and regionally diverging dynamics of coastal ecosystems. *Proc. R Soc. B.* **289**, 20212772 (2022).
21. Lara, C. et al. Coastal biophysical processes and the biogeography of rocky intertidal species along the south-eastern Pacific. *J. Biogeogr.* **46** (2), 420–431 (2019).
22. Tapia, F. J., Largier, J. L., Castillo, M., Wieters, E. A. & Navarrete, S. A. Latitudinal discontinuity in thermal conditions along the nearshore of central-northern Chile. *PLoS ONE.* **9** (10), 1–11 (2014).
23. Aguirre, C., García-Loyola, S., Testa, G., Silva, D. & Farias, L. Insight into anthropogenic forcing on coastal upwelling off south-central Chile. *Elem. Sci. Anth.* **6** (1), 59 (2018).
24. Morales, C. E., Hormazabal, S., Andrade, I. & Correa-Ramirez, M. A. Time-space variability of chlorophyll-a and associated physical variables within the region off Central-Southern Chile. *Remote Sens.* **5** (11), 5550–5571 (2013).
25. Weidberg, N. et al. Spatial shifts in productivity of the coastal ocean over the past two decades induced by migration of the Pacific Anticyclone and Bakun effect in the Humboldt Upwelling Ecosystem. *Glob Planet. Change.* **193**, 103259 (2020).
26. Camus, P. A. Biogeografía marina de Chile continental. *Rev. Chil. Hist. Nat.* **74** (3), 587–617 (2001).
27. Cárdenas, L., Castilla, J. C. & Viard, F. A phylogeographical analysis across three biogeographical provinces of the south-eastern Pacific: the case of the marine gastropod *Concholepas concholepas*. *J. Biogeogr.* **36** (5), 969–981 (2009).
28. Haye, P. A. et al. Phylogeographic structure in benthic marine invertebrates of the southeast pacific coast of Chile with differing dispersal potential. *PLoS ONE.* **9** (2), 1–15 (2014).
29. Zakas, C., Binford, J., Navarrete, S. A. & Wares, J. P. Restricted gene flow in Chilean barnacles reflects an oceanographic and biogeographic transition zone. *Mar. Ecol. Prog. Ser.* **394**(2), 165–177 (2009).
30. Sánchez, R., Sepúlveda, R. D., Brante, A. & Cárdenas, L. Spatial pattern of genetic and morphological diversity in the direct developer *Acanthina Monodon* (Gastropoda: Mollusca). *Mar. Ecol. Prog Ser.* **434**, 121–131 (2011).
31. Broitman, B. R., Navarrete, S. A., Smith, F. & Gaines, S. D. Geographic variation of southeastern pacific intertidal communities. *Mar. Ecol. Prog Ser.* **224**, 21–34 (2001).
32. Broitman, B. R., Aguilera, M. A., Lagos, N. A. & Lardies, M. A. Phenotypic plasticity at the edge: contrasting population-level responses at the overlap of the leading and rear edges of the geographical distribution of two Scurria limpets. *J. Biogeogr.* **45** (10), 2314–2325 (2018).
33. Broitman, B. R. et al. Phenotypic plasticity is not a cline: thermal physiology of an intertidal barnacle over 20° of latitude. *J. Anim. Ecol.* **90** (8), 1961–1972 (2021).
34. Wieters, E. A., Broitman, B. R. & Brancha, G. M. Benthic community structure and spatiotemporal thermal regimes in two upwelling ecosystems: comparisons between South Africa and Chile. *Limnol. Oceanogr.* **54** (4), 1060–1072 (2009).

35. Boulanger, E. et al. Climate differently influences the genomic patterns of two sympatric marine fish species. *J. Anim. Ecol.* **91** (6), 1180–1195 (2022).
36. Bird, C. E., Holland, B. S., Bowen, B. W. & Toonen, R. J. Contrasting phylogeography in three endemic hawaiian limpets (*Cellana* spp.) with similar life histories. *Mol. Ecol.* **16** (15), 3173–3186 (2007).
37. Lesson, R. P. *Voyage autour du monde, sur la Corvette la Coquille, pendant les années 1822, 1823, 1824 et 1825* - Zoologie, vol 2 (Arthus-Bertrand, (1830).
38. Orbigny, A. D. Voyage dans l'Amérique méridionale. *Mollusques (France)*. **5**, 409–488 (1841).
39. Espoz, C., Lindberg, D. R., Castilla, J. C. & Simison, W. B. Los patelogastrópodos intermareales de Chile Y Perú. *Rev. Chil. Hist. Nat.* **77** (2), 257–283 (2004).
40. Ríoz Cardoza, C. F. *Dinámica del asentamiento larvario de Scurria scurra (Lesson, 1830) (Gastropoda: Acmaeidae) en el intermareal rocoso de Mehuín (X Región)*. Master dissertation, Facultad de Ciencias, Universidad Austral de Chile (1992).
41. Kay, M. C. & Emlet, R. B. Laboratory spawning, larval development, and metamorphosis of the limpets *Lottia digitalis* and *Lottia asmi* (Patellogastropoda, Lottiidae). *Invertebr Biol.* **121** (1), 11–24 (2002).
42. Kolbin, K. G. & Kulikova, V. A. Reproduction and larval development of the limpet *Lottia persona* (Rathke, 1833) (Gastropoda: Lottiidae). *Russ J. Mar. Biol.* **37** (3), 239–242 (2011).
43. Kuo, E. S. L. & Sanford, E. Northern distribution of the seaweed limpet *Lottia insessa* (Mollusca: Gastropoda) along the Pacific Coast. *Pac. Sci.* **67** (2), 303–313 (2013).
44. Page, L. R. Apical sensory organ in larvae of the patellogastropod *Tectura scutum*. *Biol. Bull.* **202** (1), 6–22 (2002).
45. Asorey, C. M. *Diversificación y coexistencia de Lottidae (Mollusca: Patellogastropoda) en la costa del Pacífico Suroriental*. PhD thesis, Universidad Católica del Norte, Chile (2017).
46. Peluso, L., Broitman, B. R., Lardies, M. A., Nespolo, R. F. & Saenz-Agudelo, P. Comparative population genetics of congeneric limpets across a biogeographic transition zone reveals common patterns of genetic structure and demographic history. *Mol. Ecol.* **32** (14), 3812–3825 (2023).
47. Aguilera, M. A. The functional roles of herbivores in the rocky intertidal systems in Chile: a review of food preferences and consumptive effects. *Rev. Chil. Hist. Nat.* **84**, 241–261 (2011).
48. Catchen, J., Hohenlohe, P. A., Bassham, S., Amores, A. & Cresko, W. A. Stacks: an analysis tool set for population genomics. *Mol. Ecol.* **22** (11), 3124–3140 (2013).
49. Danecek, P. et al. The variant call format and VCFtools. *Bioinformatics*. **27** (15), 2156–2158 (2011).
50. O'Leary, S. J., Puritz, J. B., Willis, S. C., Hollenbeck, C. M. & Portnoy, D. S. These aren't the loci you're looking for: principles of effective SNP filtering for molecular ecologists. *Mol. Ecol.* **27** (16), 3193–3206 (2018).
51. Zheng, X. et al. A high-performance computing toolset for relatedness and principal component analysis of SNP data. *Bioinformatics*. **28** (24), 3326–3328 (2012).
52. Jombart, T. & Ahmed, I. Adegenet 1.3-1: new tools for the analysis of genome-wide SNP data. *Bioinformatics*. **27** (21), 3070–3071 (2011).
53. Frichot, E. & François, O. LEA: an R package for landscape and ecological association studies. *Methods Ecol. Evol.* **6**, 925–929 (2015).
54. Assis, J. et al. Bio-ORACLE v2.0: extending marine data layers for bioclimatic modelling. *Glob Ecol. Biogeogr*. **27** (3), 277–284 (2017).
55. Fick, S. E. & Hijmans, R. J. WorldClim 2: new 1km spatial resolution climate surfaces for global land areas. *Int. J. Climatol*. **37** (12), 4302–4315 (2017).
56. Bosch, S. & Fernandez, S. sdmpredictors: species distribution modelling predictor datasets. R package version 0.2.11. (2021). https://CRAN.R-project.org/package=sdmpredictors
57. Hijmans, R. J. raster: geographic data analysis and modeling. R package version 3.5–11. (2021). https://CRAN.R-project.org/package=raster
58. Risien, C. M. & Chelton, D. B. A global climatology of surface wind and wind stress fields from eight years of QuikSCAT scatterometer data. *J. Phys. Oceanogr.* **38** (11), 2379–2413 (2008).
59. Carton, J. A. & Giese, B. S. A reanalysis of ocean climate using simple Ocean Data assimilation (SODA). *Mon Weather Rev.* **136** (8), 2999–3017 (2008).
60. Paris, C. B., Helgers, J., van Sebille, E. & Srinivasan, A. Connectivity modeling system: a probabilistic modeling tool for the multi-scale tracking of biotic and abiotic variability in the ocean. *Environ. Model. Softw.* **42**, 47–54 (2013).
61. Burgess, S. C. et al. Beyond connectivity: how empirical methods can quantify population persistence to improve marine protected-area design. *Ecol. Appl.* **24** (2), 257–270 (2014).
62. Lett, C., Nguyen-Huu, T., Cuif, M., Saenz-Agudelo, P. & Kaplan, D. M. Linking local retention, self-recruitment, and persistence in marine metapopulations. *Ecology*. **96** (8), 2236–2244 (2015).
63. Kaplan, D. M. et al. Uncertainty in empirical estimates of marine larval connectivity. *ICES J. Mar. Sci.* **74** (6), 1723–1734 (2017).
64. Jacobi, M. N., André, C., Döös, K. & Jonsson, P. R. Identification of subpopulations from connectivity matrices. *Ecography*. **35** (11), 1004–1016 (2012).
65. Revelle, W. *psych: Procedures for Personality and Psychological Research*, Northwestern University, Evanston, Illinois, USA. R package version 2.1.9 (2021). https://CRAN.R-project.org/package=psych
66. Blanchet, F. G., Legendre, P. & Borcard, D. Modelling directional spatial processes in ecological data. *Ecol. l Model.* **215** (4), 325–336 (2008).
67. Dray, S. et al. adespatial: multivariate multiscale spatial analysis. R package version 0.3–14. (2021). https://github.com/sdray/adespatial
68. Blanchet, F. G., Legendre, P. & Borcard, D. Forward selection of explanatory variables. *Ecology*. **89** (9), 2623–2632 (2008).
69. Oksanen, J. et al. *vegan: Community Ecology Package*. R package version 2.5-7. (2020). https://CRAN.R-project.org/package=vegan
70. Forester, B. R., Lasky, J. R., Wagner, H. H. & Urban, D. L. Comparing methods for detecting multilocus adaptation with multivariate genotype–environment associations. *Mol. Ecol.* **27** (9), 2215–2233 (2018).
71. Saenz-Agudelo, P. et al. Population genomic analyses reveal hybridization and marked differences in genetic structure of Scurria limpet sister species with parapatric distributions across the South Eastern Pacific. *Ecol. Evol.* **12** (5), 1–13 (2022).
72. Fraser, C. I., Thiel, M., Spencer, H. G. & Waters, J. M. Contemporary habitat discontinuity and historic glacial ice drive genetic divergence in Chilean kelp. *BMC Evol. Biol.***10** (1), 1–12 (2010).
73. Quesada-Calderón, S., Giles, E. C., Morales-González, S. & Saenz-Agudelo, P. Pinpointing genetic breaks in the southeastern Pacific: Phylogeography and genetic structure of a commercially important tunicate. *J. Biogeogr.* **48** (10), 2604–2615 (2021).
74. Fernandez, M. et al. Diversity, dynamics and biogeography of Chilean benthic nearshore ecosystems: an overview and guidelines for conservation. *Rev. Chil. Hist. Nat.* **73**, 797–830 (2000).
75. Brattström, H. & Johanssen, A. Ecological and regional zoogeography of the marine benthic fauna of Chile. *Sarsia*. **68** (4), 289–339 (1983).
76. Spalding, M. D. et al. Marine ecoregions of the world: a bioregionalization of coastal and shelf areas. *BioScience*. **57** (7), 573–583 (2007).
77. Brante, A., Fernandez, M. & Viard, F. Phylogeography and biogeography concordance in the marine gastropod *Crepipatella dilatata* (Calyptraeidae) along the southeastern Pacific coast. *J. Hered.* **103**(5), 630–637 (2012).

78. Ibáñez, C. M. & Poulin, E. Genetic structure and diversity of squids with contrasting life histories in the Humboldt current. *Hidrobiológica* **24**(1), 1–10 (2014).
79. Segovia, N. I., Gallardo-Escárate, C., Poulin, E. & Haye, P. A. Lineage divergence, local adaptation across a biogeographic break, and artificial transport, shape the genetic structure in the ascidian *Pyura chilensis*. *Sci. Rep.* **7**, 1–12 (2017).
80. Dauphin, B. et al. Re-thinking the environment in landscape genomics. *Trends Ecol. Evol.* **38** (3), 261–274 (2023).
81. Fraser, C. I., Velásquez, M., Nelson, W. A., Macaya, E. C. & Hay, C. H. The biogeographic importance of buoyancy in macroalgae: a case study of the southern bull-kelp genus *Durvillaea* (Phaeophyceae), including descriptions of two new species. *J. Phycol.* **56** (1), 23–36 (2020).
82. González, A. et al. Identification of cryptic species in the *Lessonia Nigrescens* complex (Phaeophyceae, Laminariales). *J. Phycol.* **48** (5), 1153–1165 (2012).
83. Tellier, F., Tapia, J., Faugeron, S., Destombe, C. & Valero, M. The *Lessonia nigrescens* species complex (Laminariales, Phaeophyceae) shows strict parapatry and complete reproductive isolation in a secondary contact zone. *J. Phycol.* **47** (4), 894–903 (2011).
84. López, B. A. *et al.* Epibiont communities on stranded kelp rafts of *Durvillaea Antarctica* (Fucales, Phaeophyceae) - Do positive interactions facilitate range extensions?. *J. Biogeogr.* **45**(8), 1833–1845 (2018).
85. García-Ramos, G. & Kirkpatrick, M. Genetic models of adaptation and gene flow in peripheral populations. *Evolution*. **51** (1), 21–28 (1997).

Acknowledgements

We acknowledge financial support from Agencia Nacional Investigación y Desarrollo ANID (grants: FONDECYT 1190710, 1221699 and 1200636), Millenium Nucleus NUTME (ANID NCN2023_004), and Millennium Institute SECOS (ANID ICN2019_015). L. P. acknowledges the doctoral scholarship from ANID (21170187). We thank Felipe Pontigo, Paula Ramirez, Alejandra Vargas and members of the Saenz, Navarrete and Chango labs for assistance in the field and in the laboratory.

Author contributions

Conceptualization: L.P., J.F., S.A.N. and P.S.-A. Designed research: L.P., J.F., S.A.N. and P.S.-A. Performed research: L.P. and P.S.-A. Contributed new reagents or analytical tools: L.P., J.F., S.A.N., B.R.B., C.A. and P.S.-A. Analyzed data: L.P. and P.S.-A . Writing original draft: L.P. Writing, review and editing: J.F., S.A.N., B.R.B., C. A. and P.S.-A.

Declarations

Competing interests

The authors declare no competing interests.

Additional information

Supplementary Information The online version contains supplementary material available at https://doi.org/10.1038/s41598-024-72841-x.

Correspondence and requests for materials should be addressed to P.S.-A.